Atomic clocks and Atomic interferometers or using quantum laws for precision measurements

Caroline Champenois

Physique des Interactions Ioniques et Moléculaires
CNRS-Université d'Aix-Marseille

From the first to the second quantum revolution,
Peyresq, September 2021

Outline

a two-level atom in a quasi-resonant electromagnetic field

- When an electromagnetic wave is sent onto an atom and its frequency ω_L is close to one transition frequency $\omega_0 = (E_e - E_g)/\hbar$, we can focus on the transitions induced between these two levels, $|g\rangle$ and $|e\rangle$, and forget about the other levels.

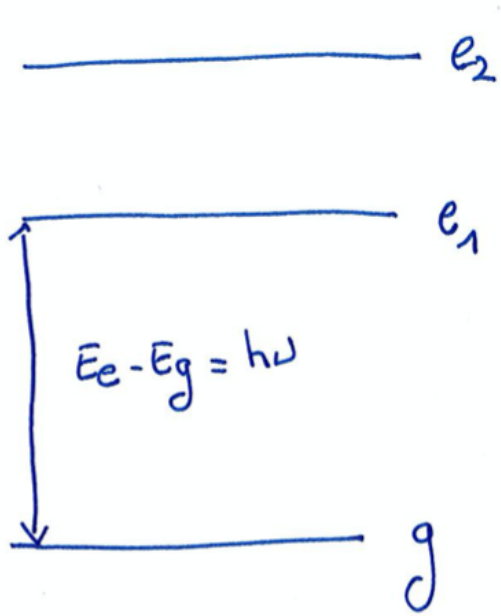

  - Depending on the frequency domain (micro-wave, optics...), the interaction between atoms and wave can be based on magnetic dipolar coupling, electric dipole coupling or even electric quadrupole coupling.

a two-level atom in a quasi-resonant electromagnetic field

- In all cases, the Hamiltonian of the coupled two-level atom can be written like

$$\hat{H} = \hbar\omega_0|e\rangle\langle e| + \hbar\Omega_1 \cos(\omega_L t + \phi)\left(|e\rangle\langle g| + |g\rangle\langle e|\right) \quad (1)$$

  where $\hbar\Omega_1 = \vec{\mu}.\vec{B}$ for a micro-wave transition and $\vec{d}.\vec{E}$ for a transition in the optical domain
- Ω_1 scales the strength of the coupling and is called the Rabi frequency.
- in an hamiltonian description, any spontaneous emission from the excited state is not accounted for and we neglect it so far.

a two-level atom in a quasi-resonant electromagnetic field

- we can then describe the internal state by any coherent combination of the two atomic eigenstates $|g\rangle$ and $|e\rangle$:

$$|\psi(t)\rangle = a_g(t)|g\rangle + a_e(t)|e\rangle. \tag{2}$$

- the time evolution is driven by the Schrodinger equation

$$i\hbar \frac{\mathrm{d}|\psi(t)\rangle}{\mathrm{d}t} = \hat{H}|\psi(t)\rangle \tag{3}$$

- without any coupling with an EM field, the free evolution by $\hbar\omega_0|e\rangle\langle e|$ makes the $a_e(t)$ coefficient rotates fast. As we are interested in the coupling effect that induces a rotation with a smaller frequency, the fast oscillation is hidden by a change in the description function :

$$a_g(t) = c_g(t) \tag{4}$$
$$a_e(t) = c_e(t)e^{-i\omega_0 t} \tag{5}$$

a two-level atom in a quasi-resonant electromagnetic field

- If $|\psi(t_0)\rangle = c_g(t_0)|g\rangle + c_e(t_0)|e\rangle$,
- after a pulse of constant EM field amplitude with length τ,

$$\begin{aligned} c_e(t_0+\tau) &= e^{-i\delta\tau/2}c_e(t_0)\left[\cos\left(\frac{\Omega\tau}{2}\right) - i\cos\theta\sin\left(\frac{\Omega\tau}{2}\right)\right] \\ &\quad + e^{-i\delta\tau/2}c_g(t_0)e^{-i(\delta t_0+\phi)}\left[-i\sin\theta\sin\left(\frac{\Omega\tau}{2}\right)\right] \\ c_g(t_0+\tau) &= e^{i\delta\tau/2}c_e(t_0)e^{i(\delta t_0+\phi)}\left[-i\sin\theta\sin\left(\frac{\Omega\tau}{2}\right)\right] \\ &\quad + e^{i\delta\tau/2}c_g(t_0)\left[\cos\left(\frac{\Omega\tau}{2}\right) + i\cos\theta\sin\left(\frac{\Omega\tau}{2}\right)\right] \quad (6) \end{aligned}$$

with $\delta = \omega_L - \omega_0$, $\Omega = \sqrt{\Omega_1^2 + \delta^2}$ and where θ is defined by

$$\sin\theta = \Omega_1/\Omega \; ; \quad \cos\theta = -\delta/\Omega \; ; \quad 0 \leq \theta < \pi. \qquad (7)$$

Some exemples of evolution after a well designed pulse

- For on resonant excitation ($\delta = 0$), if the initial state is the ground state $|g\rangle$:

$$c_e(\tau) = -i \sin\left(\frac{\Omega\tau}{2}\right) e^{-i\phi} \tag{8}$$

- the probability $P_e(\tau)$ for an atom to be in the excited state is then

$$P_e(\tau) = |c_e(\tau)|^2 = (1 - \cos(\Omega\tau))/2 \tag{9}$$

This periodic occupation of the ground and excited state is called "Rabi flopping".

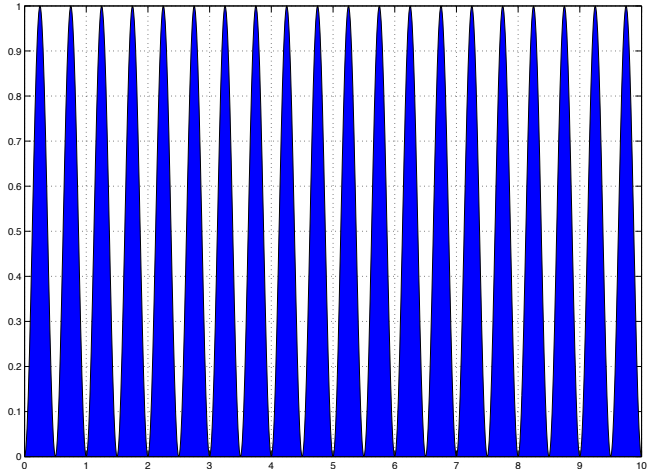

Some exemples of evolution after a well designed pulse

- A π-pulse is designed to transfer the population to the excited state with probability 1 as $\Omega\tau = \pi$.

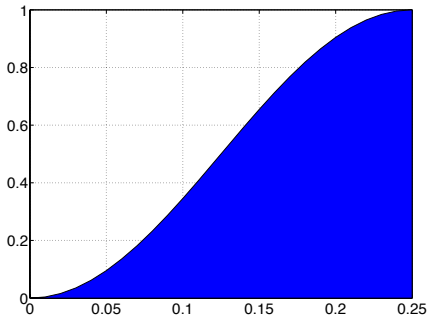

- A $\pi/2$-pulse on resonance creates a linear superposition

$$|\psi(t_0+\tau)\rangle = (|g\rangle + e^{-i\phi}(-i)|e\rangle)\sqrt{2})$$

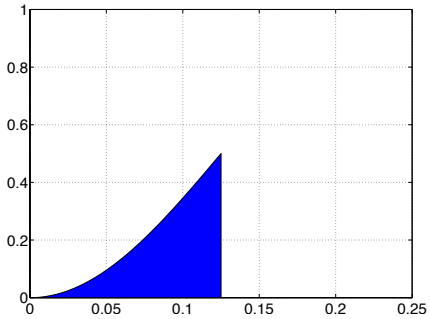

- If $\delta \neq 0$, the flopping does not reach $P_e = 1$ for any pulse duration.

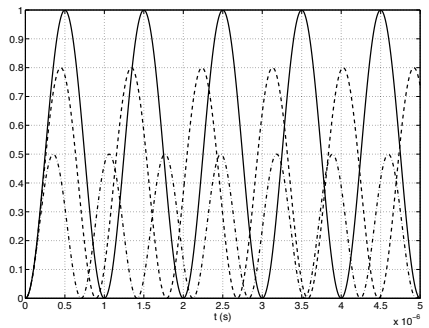

Sensitivity to the excitation detuning

- the average occupation probability in the excited state is

$$P_e^{\infty} = \frac{1}{2}\frac{\Omega_1^2/2}{(\delta^2 + \Omega_1^2/2)} \tag{10}$$

- the minimum full width at half maximum (FWHM) of the average occupation probability is due to power broadening :

$$FWHM = \sqrt{2}\Omega_1$$

- to increase the sensitivity to the field detuning, the line must be as narrow as possible, which implies an excitation strength or Rabi frequency Ω_1 as small as possible, which in turn, implies to increase the interaction time to cover many floppings or to reach a π-pulse.
- ...until the Doppler effect broadens the line also.

How to limit Doppler broadening in spectroscopy

- the first order Doppler effect is the main cause of inhomogeneous broadening

$$\omega_L^{at} = \omega_L - \vec{k}_L.\vec{v}_{at} \tag{11}$$

  and for a gas at thermodynamical equilibrium, the average velocity scales like $\sqrt{T}$.

- most of the early precision experiments run in the 50's and 60's where based on molecular beams to have $\vec{k}_L \perp \vec{v}_{at}$
- With a molecular beam, increasing the interaction duration means increasing the interaction length.

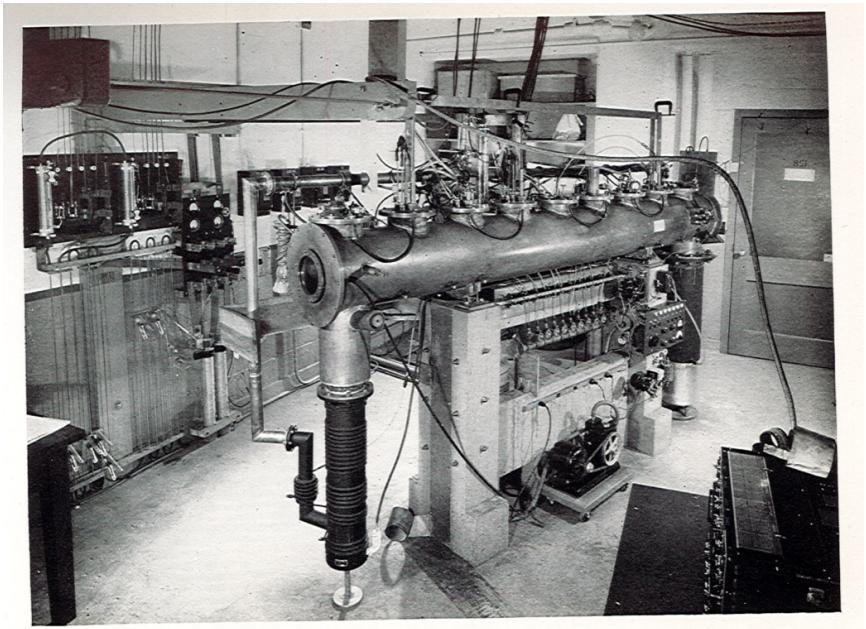

FIG. I. 2. Photograph of a typical molecular beam apparatus (KOL 50).

From "Molecular Beams", N.F. Ramsey, Oxford (1956)

The limit of a long interaction zone

- Ramsey *and coll.* were working on magnetic-dipole transition in the micro-wave domain to measure nuclear magnetic moments.

- this method requires an applied static magnetic field to align the magnetic moments and to define the energy of each atomic level.
- Then, a quasi-resonant oscillating magnetic field drives transition between these levels.

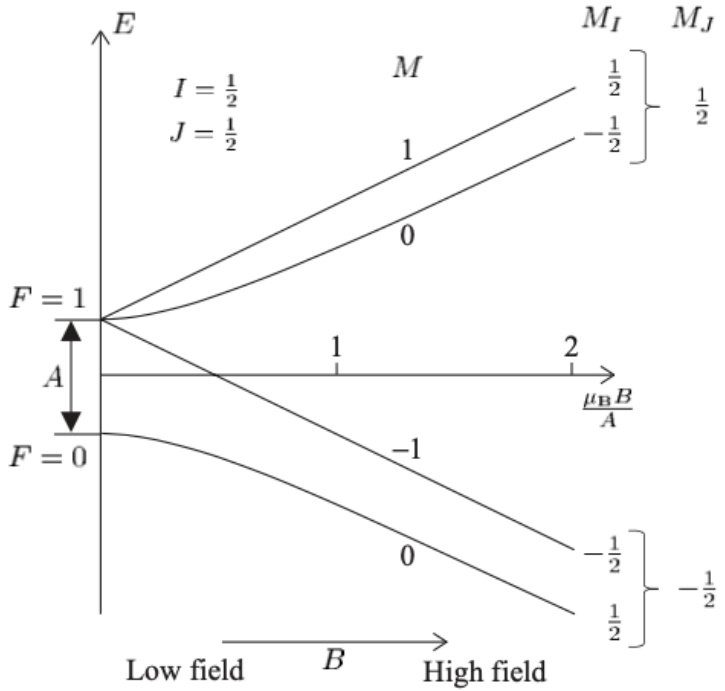

Hyperfine structure of the ground state of Hydrogen.

The limit of a long interaction zone

- the main limitation for precise measurements came from the inhomogeneity of the magnetic field as *"it is impossible in practise to achieve completely uniform magnetic fields over great lengths so the resonance frequencies differ along the length of the beam with the result that the observed resonance pattern is frequently broadened far beyond theory...with an increase rather than a decrease in width as the length l of the transition region is increased* (N. Ramsey, Molecular beams, Oxford U. P, 1956).

The Ramsey's separated oscillatory field method

- Motivated by the technical difficulties to make a long cavity with an homogeneous static magnetic field, N. Ramsey proposes in 1950 a new method for spectroscopy in the micro-wave domain, for which he received the Nobel Prize in 1989.
- the idea : having two **coherent** short interaction pulses separated by a long free flight instead of one long interaction time.

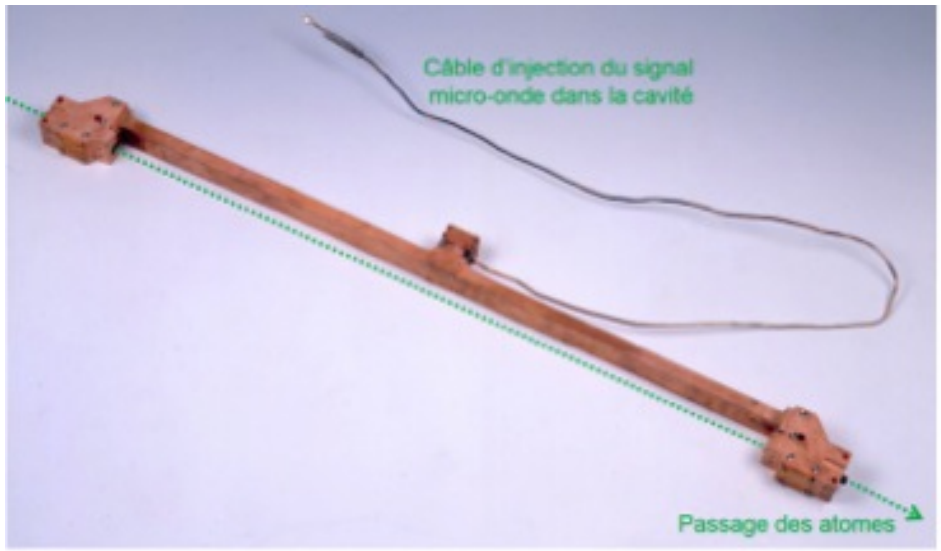

a two zone cavity for micro-wave sepctroscopy

The Ramsey's separated oscillatory field method

- If the first pulse length is chosen to be a $\pi/2$ pulse but the field is not on resonance, then $\Omega\tau = \pi/2$ and

$$c_e(\tau) = e^{-i\delta\tau/2} e^{-i\phi}(-i\sin\theta)/\sqrt{2} \quad (12)$$

$$c_g(\tau) = e^{+i\delta\tau/2}(1 + i\cos\theta)/\sqrt{2} \quad (13)$$

- this first pulse is followed by a free flight of duration T, with no interaction with any EM field.
- Then a second $\pi/2$-pulse is applied and the probability $P_e(2\tau + T)$ to find the atom in the excited state is

$$P_e(2\tau + T) = |c_e(2\tau + T)|^2 = \sin^2\theta \left[\cos\left(\frac{\delta T}{2}\right) + \cos\theta \cos\left(\frac{\delta T}{2}\right)\right]^2 \quad (14)$$

The Ramsey's separated oscillatory field method

- At the end of the second $\pi/2$-pulse

$$P_e(2\tau+T) = |c_e(2\tau+T)|^2 = \sin^2\theta\left[\cos\left(\frac{\delta T}{2}\right) + \cos\theta\cos\left(\frac{\delta T}{2}\right)\right]^2 \quad (15)$$

- For near resonance interaction, with $\delta \ll \Omega$

$$P_e(2\tau+T) \simeq (1+\cos(\delta T))/2 \quad (16)$$

the "resonance line" has a width (chosen as the detuning range for full width at half maximum-FWHM)

$$\delta_{FWHM} = \pi/T$$

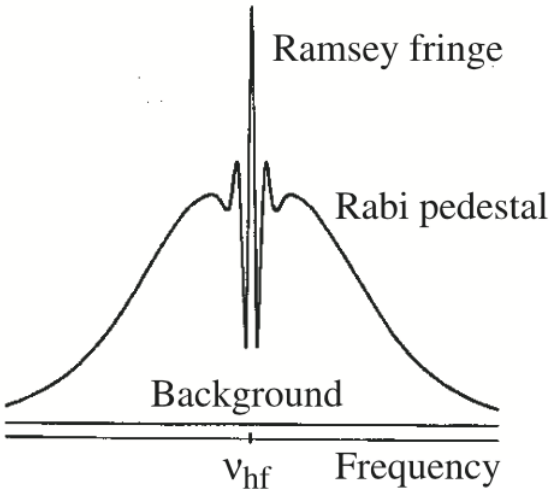

Figure 6. Ramsey pattern obtained in a short optically pumped caesium beam tube. The line width of the central fringe is 500 Hz [21].

From precision spectroscopy to the first atomic clocks

- the idea of using the sensitivity of a transition to the excitation detuning came from I. Rabi in the late 40's
- the first device ever built in this spirit was based on transition within the vibration state of the ammonia molecule, it is an active device (MASER), too unstable and abandoned.

the first atomic clock was based on a Cs beam going through a separated-field cavity of Ramsey kind. It was built in the early 50's (NBS-US and NPL-UK)

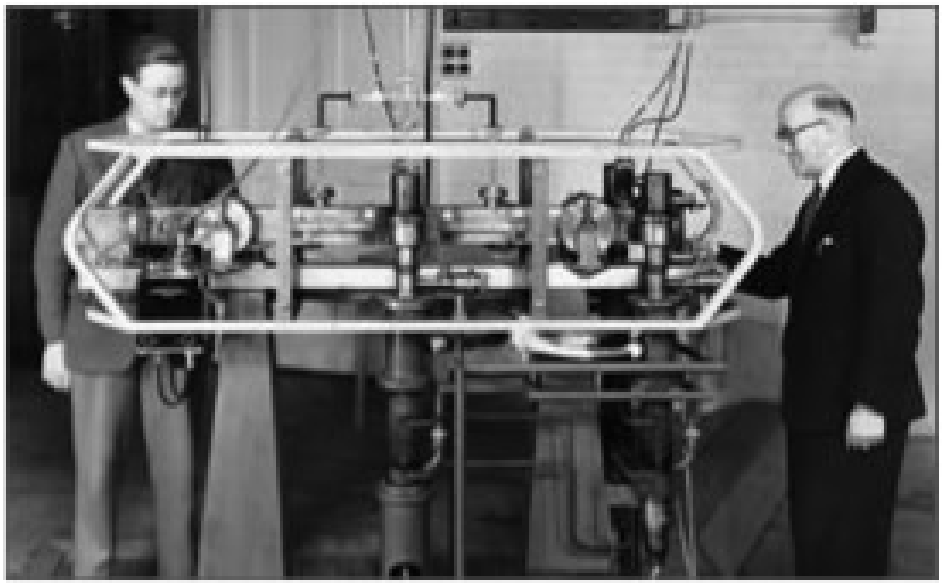

L. Essen et J. Parry. at NPL, 1955

Today's performances and applications of micro-wave atomic clocks of the Ramsey kind

- they reached their best performances at the end of the 90's in several national labs with a free flight of 1 m long.
- exemple at SYRTE : relative frequency stability $3,5 \times 10^{-13}\tau^{-1/2}$ and relative accuracy $6,4 \times 10^{-15}$.
- these performances are outcome by cold atom fountains which takes advantage of the reduced velocity of the atom (few cm/s) and of the gravity fall to increase the free flight duration.
- the best reported relative instability is $2 \times 10^{-14}\tau^{-1/2}$

Today's best micro-wave atomic clocks : the cold atom fountain

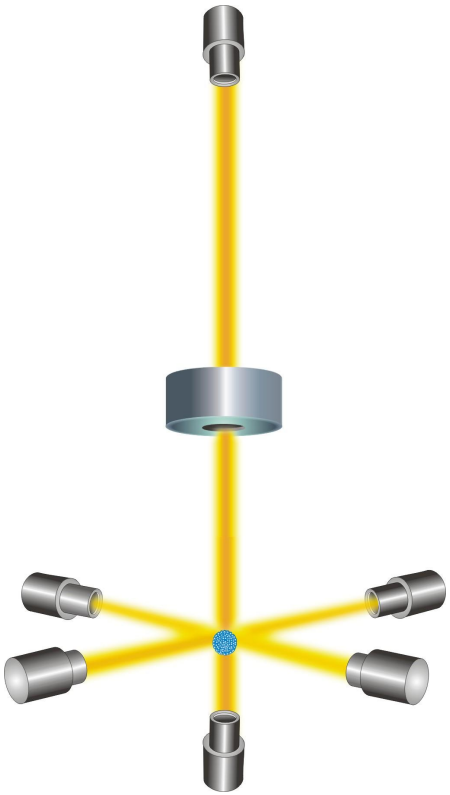

step 1 : A gas of cesium atoms enters the clock's vacuum chamber. Six lasers slow the movement of the atoms, cooling them to near absolute zero and force them into a spherical cloud at the intersection of the laser beams.

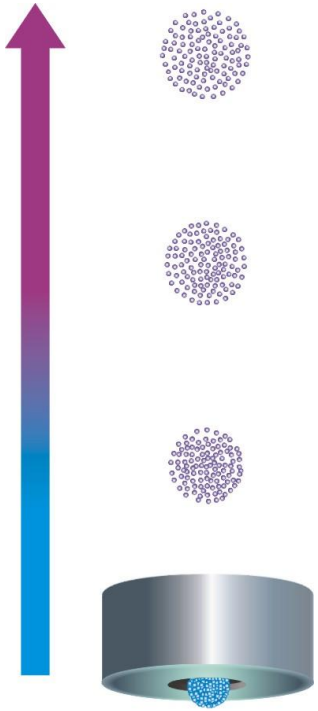

step 2 : The atom cloud is tossed upward by two lasers through a cavity filled with microwaves nearly resonant with the transition between 2 atomic states. All of the lasers are then turned off.

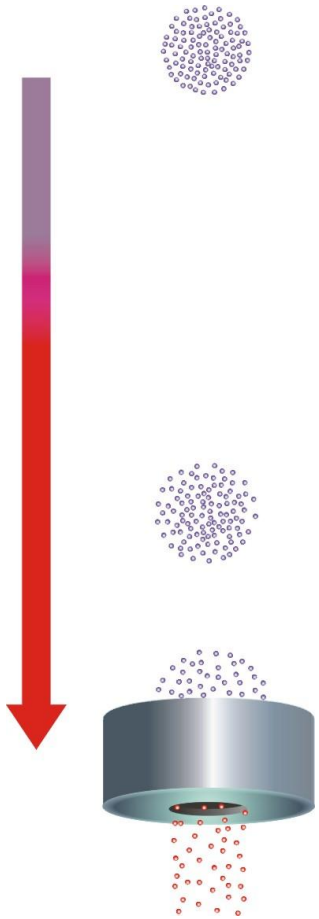

step 3 : Gravity pulls the cesium atoms back through the microwave cavity.

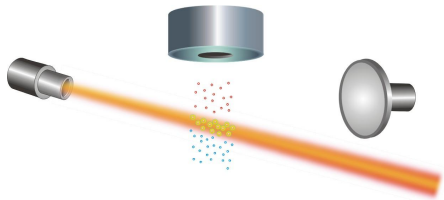

step 4 : Cesium atoms that end up in the excited state after crossing the microwave cavity emit light when excited by a laser beam. This fluorescence is measured by a detector (right). The entire process is repeated to draw the resonance profile with the Ramsey method, and lock a micro-wave synthetizer frequency on the atomic transition frequency

Today's best micro-wave atomic clocks : the cold atom fountain

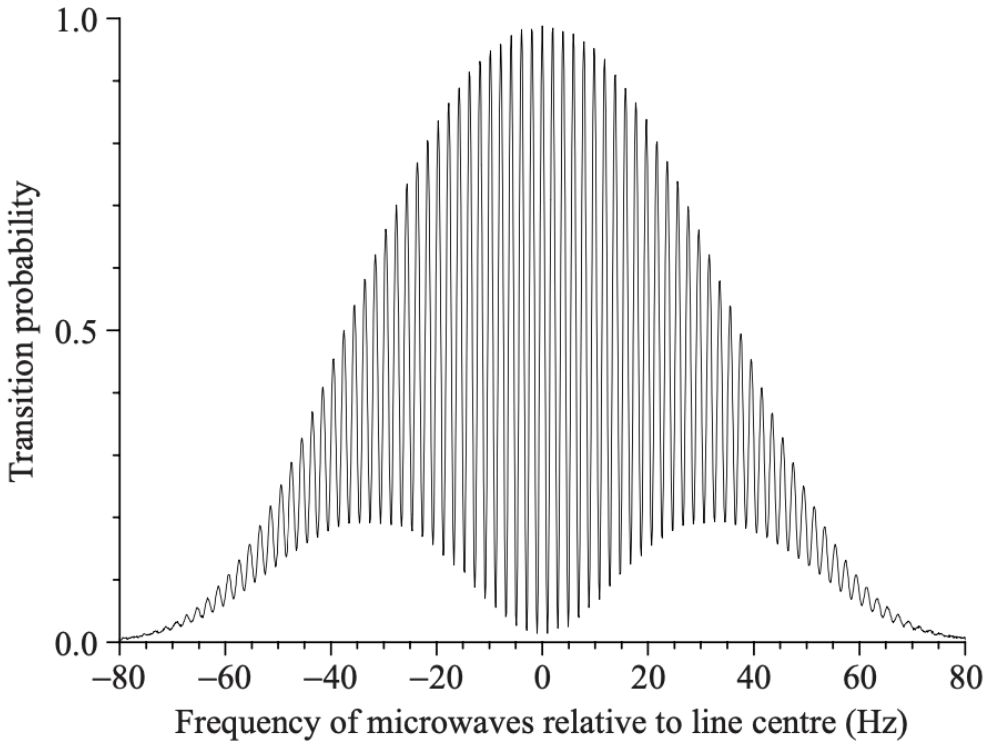

Typical atomic fountain signal for a height of 31 cm which result in a central fringe of width of the order of 1 Hz.

A cold atom fountain in space: the PHARAO project

or how to avoid the limitation induced by gravitational fall

- part of ACES: Atomic Clock Ensemble in Space: PHARAO+H-MASER for short and middle range stability.
- expected to be launched in 2021 to be settled on ISS
- ACES aims at testing of new generation of space clocks for reaching frequency instability and inaccuracy of a few parts in 10^{16}.
- the other technical challenge relies in the ability to achieve high stability on space-to-ground time and frequency transfer.
- then, the link will be used for high resolution comparisons of Ground Clocks via the ACES Microwave Link

A cold atom fountain in space: the PHARAO project

- Fundamental physics experiments will be made possible by PHARAO :
- Gravitational Red-shift. To measure with an improved accuracy the Einstein's gravitational red-shift.
- Drift of Fine Structure Constant. To measure time variations of the fine structure constant α at an increased level of accuracy.
- Anisotropy of Light. To test the validity of special relativity by detecting a possible anisotropy of the light velocity with an improved accuracy.

clocks used for global navigation satellite systems (GNSS)

- the atomic clocks launched in the latest GNSS like GALILEO are not based on the Ramsey interrogation method
- 4 clocks are present in each satellite of the GALILEO system : 2 H-MASER and 2 Rb-cell clocks
- they are chosen for their short and long-term stability, limited volume and power need.
- they all work on a continuous Rabi-scheme interrogation protocol

A micro-wave clock tested for long range navigation

- a 16-pole trap for Hg^+ ions developed at JPL (Cal Tech, Pasadena) by Prestage, Maleki, Burt and coworkers, (NASA : project LITS: Linear Ion Trap Standards)

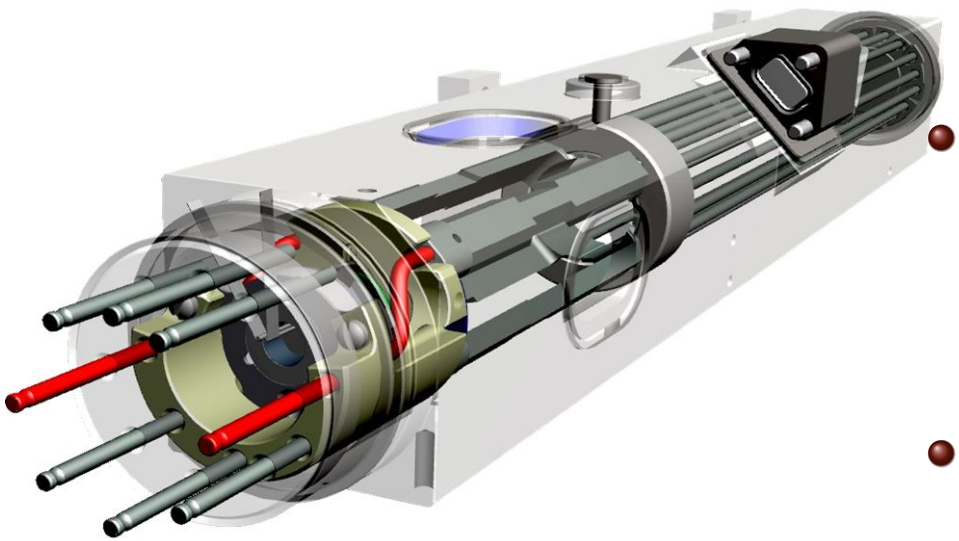

- micro-wave interrogation scheme based on a single long pulse (Rabi pulse)
- no lasers required, a lamp filled with another isotope of Hg^+ drives the optical pumping and read-out of the internal state.
- more than 10^7 ions are cooled by collisions with a Neon buffer gas at 300 K and shuttled between the two traps.

A micro-wave clock tested for long range navigation

physicsworld | Magazine | Lates

METROLOGY | RESEARCH UPDATE

Trapped-ion clock passes orbital test

03 Jul 2021

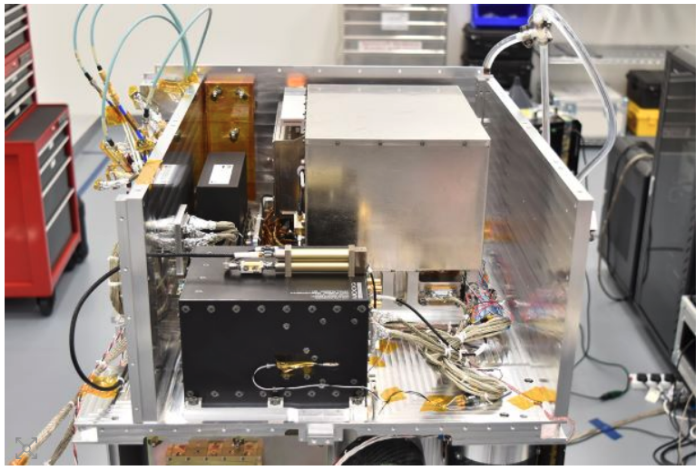

Stable ticker: The payload of the Deep Space Atomic Clock mission, which launched in 2019, includes an atomic clock, a GPS receiver, and an ultra-stable oscillator. (Courtesy: NASA)

A compact atomic clock that has orbited the Earth since 2019 is far more stable than previous space-based clocks, raising hopes that future spacecraft will be able to keep track of time autonomously. Although technical problems have limited the new trapped-ion device's performance, the US-based scientists who developed it report that it is reliable enough to substantially reduce the need for back-and-forth communication with controllers on the ground, thereby improving navigation.

A Ramsey separated field method in the time domain, or the pulsed Ramsey method

The Ramsey interrogation scheme is used in some of the clocks developed in national labs for the next generation of satellites, but the two pulses are now separated in the time domain with non-moving atoms.

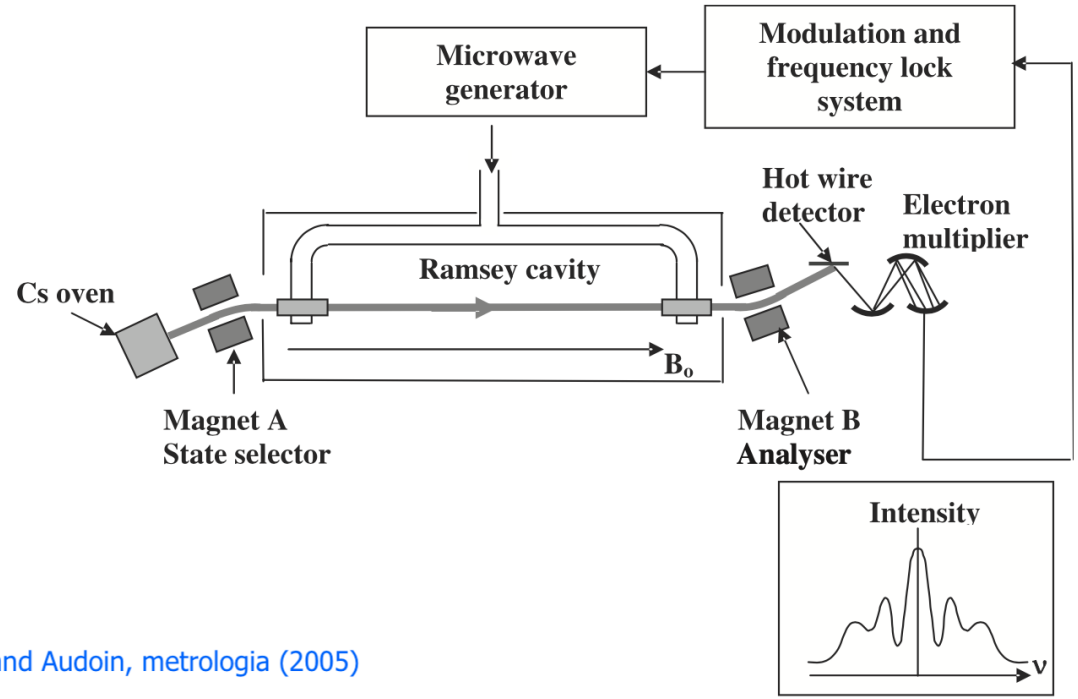

from Vanier and Audoin, metrologia (2005)

Figure 2. Simplified conceptual diagram of the Cs beam frequency standard using magnetic state selection. The inset shows the shape of the resonant signal observed when the frequency-lock loop is open and the microwave frequency is scanned slowly over the atomic hyperfine resonance. Although in the figure the magnetic induction is shown parallel to the beam direction, in practice it is very often made perpendicular to the beam.

A Ramsey separated field method in the time domain, or the pulsed Ramsey method

The Ramsey interrogation scheme is used in some of the clocks developed in national labs for the next generation of satellites, but the two pulses are now separated in the time domain with non-moving atoms.

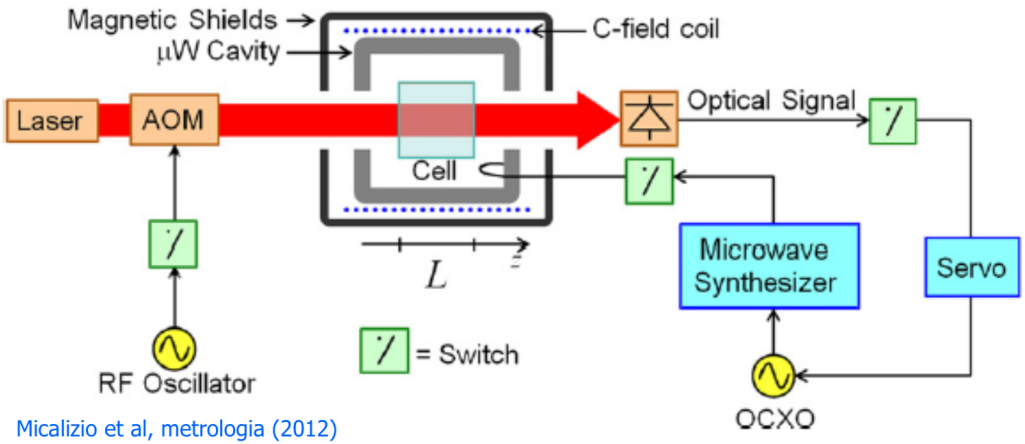

Micalizio et al, metrologia (2012)

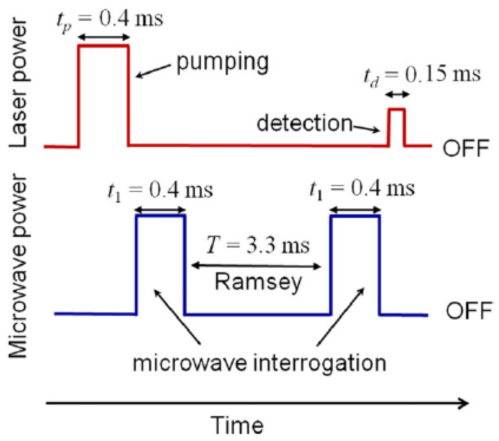

example of the INRIM pulsed optically pumped Rb clock

From micro-wave to optical clocks

motivations and feasibility

- The stability of a clock can be quantified by the Allan deviation, which behaves like

$$\sigma_y(\tau) = \frac{\Delta f}{f_0}\sqrt{\frac{1}{S/N}}\sqrt{\frac{T_c}{\tau}} \tag{17}$$

- Going from the micro-wave to the optical domain increase f_0 by 10^5
- Taking advantage of this without increasing Δf by the same amount requires to limit the Doppler effect
- It relies on the well controlled laser-atom interaction and the concept was explored already in 1976
- In 1991, several pioneer experiments open the path for high precision measurement in the optical domain

How to adapt a Ramsey method to the optical domain?

- the relevant length scale makes a big difference : the wavelength for micro-wave (3.3 cm for 9.2 GHz) is far larger than optical wavelengths which are of the order of 1 μm
- the displacement of the atoms or molecules inside the wave can not be neglected anymore.

$$V_{AL}(\mathrm{r},t) = -\mathrm{d}_{eg}.E_L(\mathrm{r})\epsilon_L \cos(\omega t - \Phi(\mathrm{r}))$$

- the role of the reduction of the motion amplitude was first demonstrated in 1952 and called the Lamb-Dicke effect

PHYSICAL REVIEW VOLUME 89, NUMBER 2 JANUARY 15, 1953

The Effect of Collisions upon the Doppler Width of Spectral Lines

R. H. Dicke
Palmer Physical Laboratory, Princeton University, Princeton, New Jersey
(Received September 17, 1952)

Quantum mechanically the Doppler effect results from the recoil momentum changing the translational energy of the radiating atom. The assumption that the recoil momentum is given to the radiating atom is shown to be incorrect if collisions are taking place. If the collisions do not cause broadening by affecting the internal state of the radiator, they result in a substantial narrowing of the Doppler broadened line.

- if $\Delta r \ll \lambda_L$, the motion has no effect and the Doppler effect is cancelled.

What does it change to move to the optical domain?

- the Doppler effect can hardly be neglected whereas there are experimental configurations where it is cancelled by the Lamb-Dicke effect in the micro-wave domain.
- another point of view : the photon recoil velocity $\vec{v}_{rec} = \hbar\vec{k}/m$ is such that its impact on the atom velocity has a signature on the atom-light interaction.
- the spontaneous emission can not be neglected for the strongest transition : the number of modes in the EM-field of the vacuum scales like $1/\lambda^3$, so typical excited state lifetime are now of the order of 10 ns instead of years...

the mechanical effect of light can not be neglected in the optical domain

Absorption and emission of light by atoms :

- if the photon energy is close enough to the energy gap between levels g and e, absorption of the photon by the atom can occur.
- if the atom was initially in its ground state, it is excited to state e, where it remains for an *average* duration τ_e. To come back to the ground state, the atom needs to give back the received energy and it emits a photon,

the mechanical effect of light can not be neglected in the optical domain

Absorption and emission of light by atoms :

- if the photon energy is close enough to the energy gap between levels g and e, absorption of the photon by the atom can occur.
- if the atom was initially in its ground state, it is excited to state e, where it remains for an *average* duration τ_e. To come back to the ground state, the atom needs to give back the received energy and it emits a photon,
  - either **spontaneously**

the mechanical effect of light can not be neglected in the optical domain

Absorption and emission of light by atoms :

- if the photon energy is close enough to the energy gap between levels g and e, absorption of the photon by the atom can occur.
- if the atom was initially in its ground state, it is excited to state e, where it remains for an *average* duration τ_e. To come back to the ground state, the atom needs to give back the received energy and it emits a photon,
  - either **spontaneously**
  - or by **stimulated emission**, if the driving by the EM wave is strong

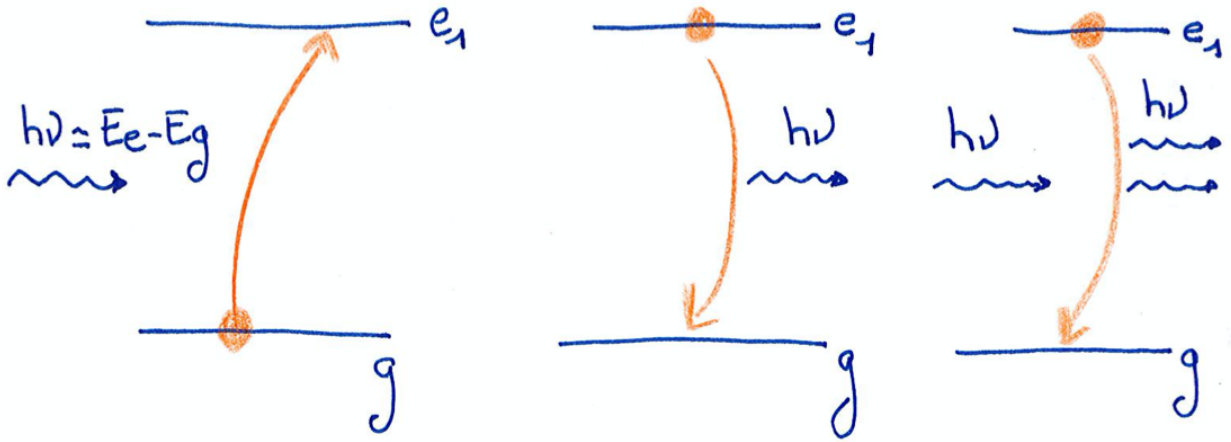

enough

the mechanical effect of light can not be neglected in the optical domain

Absorption and emission of light by atoms :

- if the photon energy is close enough to the energy gap between levels g and e, absorption of the photon by the atom can occur.
- if the atom was initially in its ground state, it is excited to state e, where it remains for an *average* duration τ_e. To come back to the ground state, the atom needs to give back the received energy and it emits a photon,
  - either **spontaneously**
  - or by **stimulated emission**, if the driving by the EM wave is strong enough
- these two emission processes result in different wave vector direction :

the mechanical effect of light can not be neglected in the optical domain

Absorption and emission of light by atoms :

- if the photon energy is close enough to the energy gap between levels g and e, absorption of the photon by the atom can occur.
- if the atom was initially in its ground state, it is excited to state e, where it remains for an *average* duration τ_e. To come back to the ground state, the atom needs to give back the received energy and it emits a photon,
  - either **spontaneously**
  - or by **stimulated emission**, if the driving by the EM wave is strong enough
- these two emission processes result in different wave vector direction :
  - on random direction for spontaneous processes.
  - in the direction of the driving EM wave for stimulated processes.

the mechanical effect of light

A photon carries energy **and** momentum $\hbar\vec{k}$

- there is a recoil induced by one photon absorption, $v_{rec} = \hbar k/m$.
- order of magnitude for optical resonance line :
  $v_{rec} = 3$ m/s for hydrogen and 3.5 mm/s for caesium,

the mechanical effect of light

A photon carries energy **and** momentum $\hbar\vec{k}$

- there is a recoil induced by one photon absorption, $v_{rec} = \hbar k/m$.
- order of magnitude for optical resonance line : $v_{rec} = 3$ m/s for hydrogen and 3.5 mm/s for caesium,
- if the photon emission is stimulated, the net gain in recoil is null for one absorption/emission cycle. This is a Rabi flopping with no change in the motion state of the atom.

What does it change in a Ramsey scheme?

- the description of the atomic state by its only internal state is not sufficient anymore. Furthermore, if the atoms have a very low velocity, the de Broglie wavelength $\lambda_{dB} = h/(mv)$ is not negligible compared to the optical wavelength and a semi-classical description of the "position of the atom relative to the EM-wave" breaks down.
- the eigenstate that are coupled by the Rabi pulses are now

$$|g, \vec{p}\rangle \quad ; \quad |e, \vec{p} + \hbar\vec{k}\rangle$$

What does it change in a Ramsey scheme?

- the time evolution of the ket can now be written like

$$|\psi(t)\rangle = c_{g,p}|g,\vec{p}\rangle e^{-i\left(\frac{|p|^2}{2m\hbar}\right)t} + c_{e,p+\hbar k}|e,\vec{p}+\hbar\vec{k}\rangle e^{-i\left(\omega_0+\frac{|p+\hbar k|^2}{2m\hbar}\right)t} \tag{18}$$

- the detuning is now

$$\delta = \omega_L - \left(\omega_0 + \frac{\vec{p}.\vec{k}}{m} + \frac{\hbar k^2}{2m}\right) \tag{19}$$

The $\pi/2$ pulse acts as a beam splitter. After a time T, the spatial separation between the two wave packets $v_{rec} \times T$ can reach millimeters for slowed down atomic beam. The two wave-packets do not overlap after the second $\pi/2$ pulse and there is no signal coming from their common contribution.

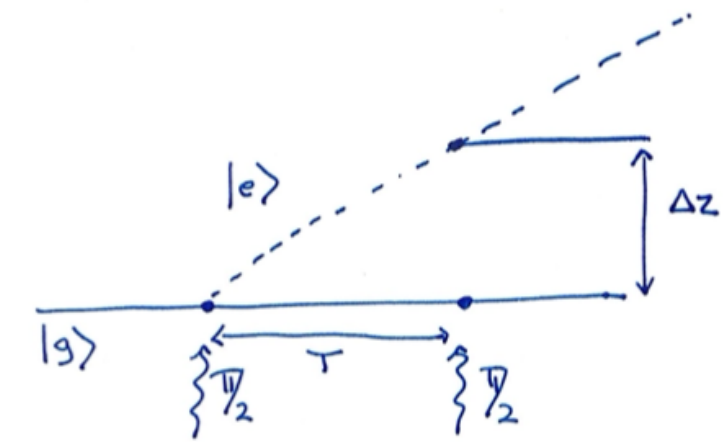

The simplest way to have overlapped wave-packet : the Mach-Zehnder interferometer

- first demonstrated by Kasevich and Chu in 1991

- after a time T, a π pulse acts as a mirror so that they overlap at time $2T$ of the second $\pi/2$ pulse.

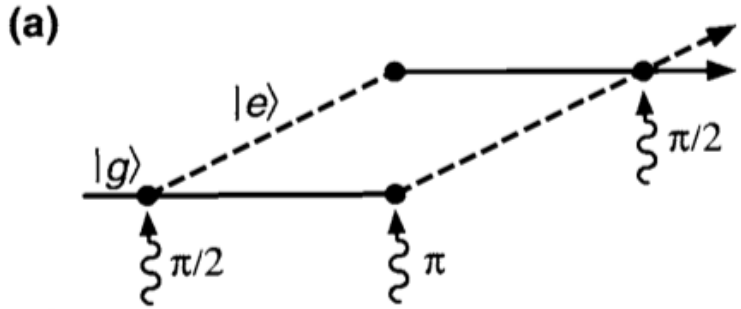

- this recoil diagram uses the vertical axis as the position z of the atom relative to a reference frame freely falling along the initial trajectory of the atom.
- closing an interferometer turns it into an achromatic IFM, so all the atoms contribute to the same signal, independently of their velocity. If not, the contributions of all the atoms blur the signal.

Avoiding the spontaneous emission

- the lifetime of the excited state must be longer than the time of flight to go through the interferometer, which is of the order of 10 ms.
- one solution is to chose a metastable state as an excited state : limited number of option, but relevant for Ramsey-type optical clock

- another solution is to use a standing wave as a beam-splitter and mirrors. the net recoil is $\hbar\vec{k}_{eff} = 2 \times \hbar\vec{k}_1$ but the internal states are not labelled
- to keep a labelled state : Raman transition between 2 sub-levels of the ground state with a net recoil $\hbar\vec{k}_{eff} = \hbar(\vec{k}_1 - \vec{k}_2)$.

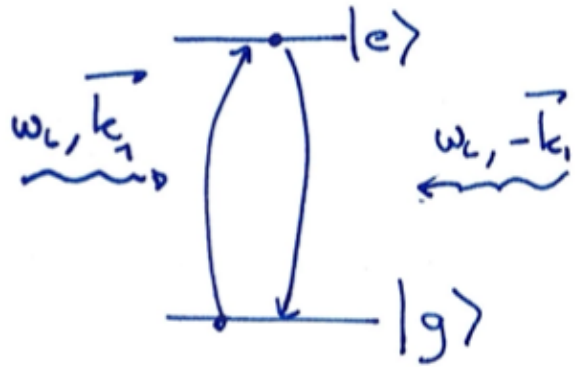

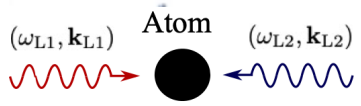

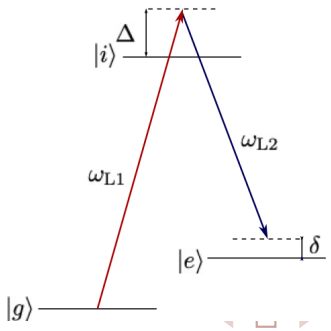

from the four wave optical Ramsey geometry to the Ramsey-Bordé interferometer

- Extending the concept of Ramsey spectroscopy to the optical domain was proposed already in 1976 and first experiments were run in the 80's at the PTB, with a closed path design using 4 traveling waves nearly resonant with a transition to a metastable state of Mg and Ca.

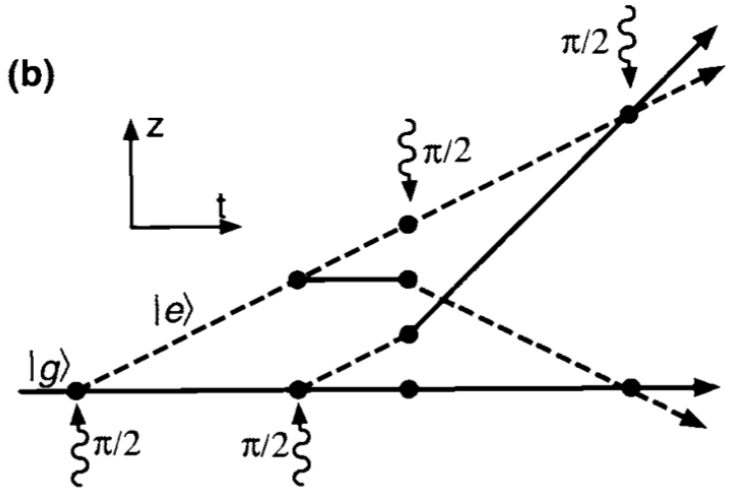

- its understanding as a 4 pulses interferometer was discovered years later, in 1982, by Bordé. This new understanding opened the way to many more applications

Phases involved in the interference signal in the Mach-Zehnder configuration

- We assume nearly resonant pulses ($|\delta| \ll \Omega_1$) and assume that all the applied pulses have the same coupling strength Ω_1.

$\pi/2$ pulse at time t_1,
π pulse at time $t_2 = t_1 + T + \tau/2$,
$\pi/2$ pulse at time
$t_3 = t_1 + 2T + 3\tau/2$

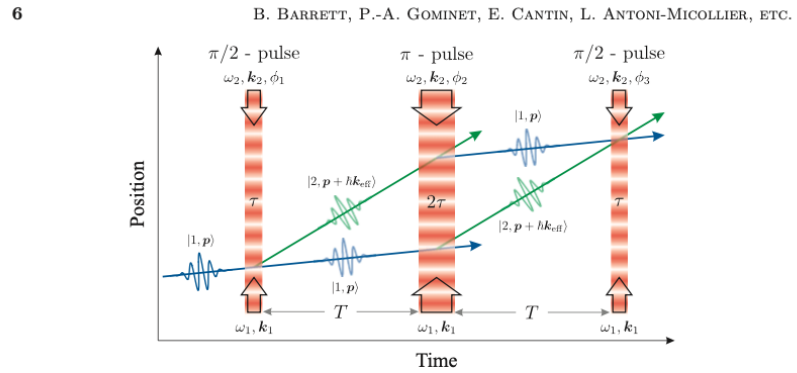

Fig. 2. – (Colour online) Three-pulse atom interferometer based on stimulated Raman transitions. Here, $\boldsymbol{k}_{\rm eff} = \boldsymbol{k}_1 + \boldsymbol{k}_2$ is the effective wave vector for the two-photon transition, and the pulse duration τ is defined by $\Omega_{\rm eff}\tau = \pi/2$. arXiv 1311.7033

$$c_{e,p+\hbar k} = -i/2 e^{-i\delta\tau/2} e^{-i(\delta t_2 + \Phi(t_2))} (1 - e^{i\delta\tau/2} e^{-i\Delta\Phi})$$

where, at each time t_i, $\Phi(t_i) = \vec{k_i}.\vec{r_i} + \phi_i$ is the phase of the light, relative to the atom, referenced to the phase at some fixed time point:

$$\Delta\Phi = \Phi(t_1) - 2\Phi(t_2) + \Phi(t_3)$$

Phases involved in the interference signal in the Mach-Zehnder configuration

- for labelled state IFM, the signal is based on the probability of finding the atom in the excited state :

$$P_{e,p+\hbar k}(2T+2\tau) = (1-\cos(\Delta\Phi - \delta\tau/2))/2 \qquad (20)$$

- the phase of the light field at the times of interaction are imprinted onto the atomic wave function, and $\Delta\Phi$ depends on the relative atom position at the different time t_i :
- It does not explicitly depends on the atom velocity, so all the atoms contribute to the same signal.
- the sensitivity to δ makes this set-up also relevant to serve as a clock basis but with thermal beam, the coherence length limits the number of visible fringes : $x_{coh} \equiv \hbar/(2\Delta p)$.

Phases in a pulsed Mach-Zehnder (MZ) configuration

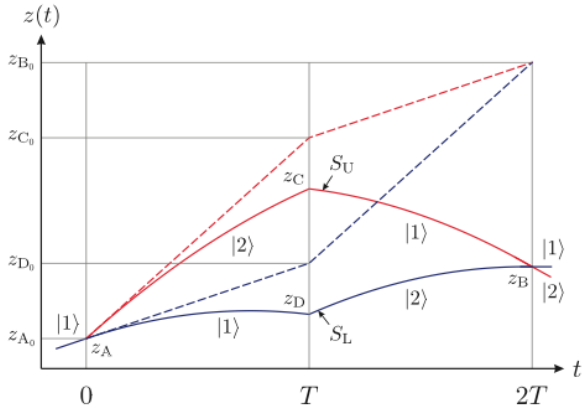

Fig. 4. – (Colour online) Center-of-mass trajectories taken by the atoms in a Mach-Zehnder interferometer with gravity (dashed lines) and without gravity (solid lines). arXiv 1311.7033

- the atomic population is changed if the phase of the pulses relative to the atom is changed : this effect is the basis for inertial force measurements and photon-recoil measurement.
- for the pulsed MZ configuration with vertical laser beams

$$\Delta\Phi = k_{eff}(z_1 - 2z_2 + z_3) + (\phi_1 - 2\phi_2 + \phi_3) \text{ and } z_2 - z_1 = z_3 - z_2 = -\frac{1}{2}gT^2$$

$$\Delta\Phi = -k_{eff}gT^2 + (\phi_1 - 2\phi_2 + \phi_3)$$

An exemple of the earliest results with a MZ geometry

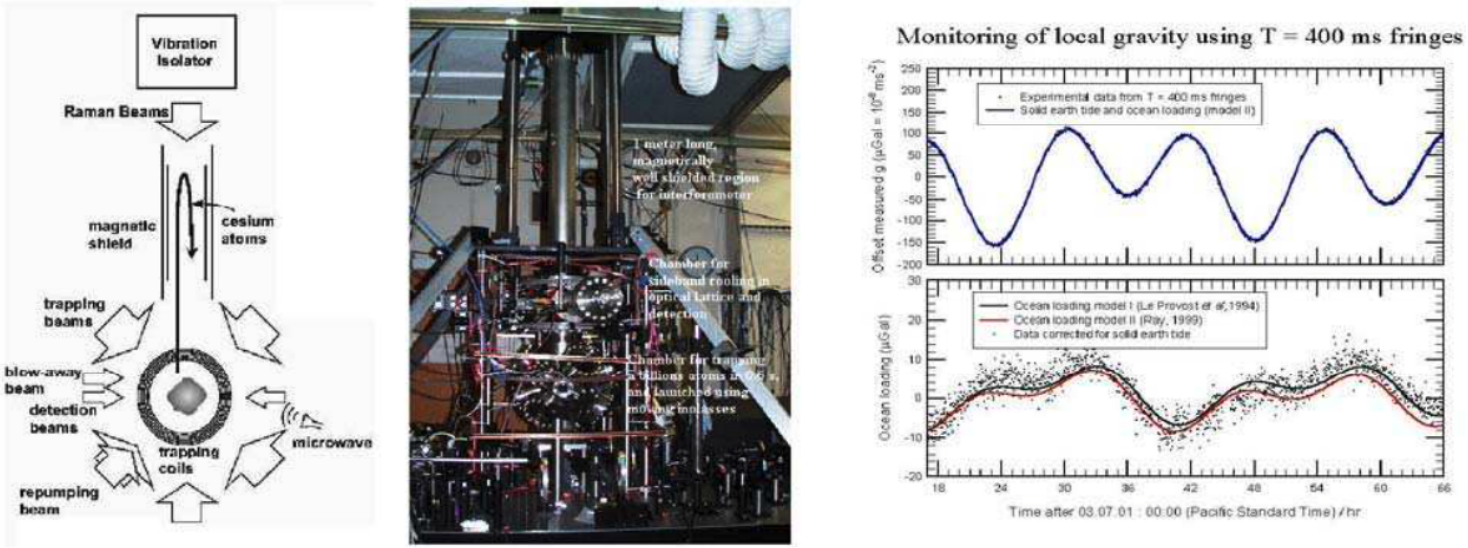

Fig. 9. – (Colour online) The atomic-fountain-based gravimeter developed by the Chu group at Stanford during the 1990's [19, 52, 39]. On the right is a two-day recording of the variation of gravity. The high accuracy enables ocean loading effects to be observed. Photo courtesy of S. Chu and M. Kasevich.

arXiv 1311.7033

How the measurement run in practise

- the change in the Doppler shift induced by the free fall requires to tune the Raman beam frequency to remain on resonance
- in practise, the effective frequency $\Delta\omega = \omega_1 - \omega_2$ is chirped with a phase-continuous sweep:

$$\Delta\omega(t) = \omega_0 + \beta(t - t_0)$$

- then, the effective interferometer phase is

$$\Delta\Phi = (\beta - k_{eff}\, g)\, T^2$$

- in the Kasevich and Chu experiment, $T \simeq 100$ ms and the 2 photon recoil $\simeq 6$ cm/s so the wave-packets are separated by 6 mm.
- when $\beta = k_{eff}\, g \pm 2\pi / T^2$ the signal is maximal, the central fringe is identified because it does not depend on T.

An exemple of the today's results with a MZ geometry

INSTITUT d'OPTIQUE GRADUATE SCHOOL

APPLICATIONS TO GEOPHYSICS

cnrs

université de BORDEAUX

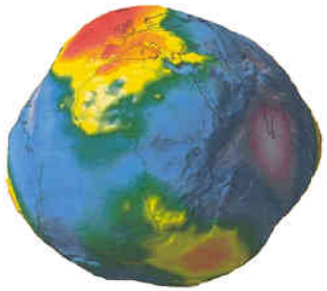

- **Applications to geophysics**
  - **Recording the time variations of gravity**
  - **Observation of tides, but also volcano survey, water cycle …**

Groupe de A. Landragin, LNE-SYRTE.

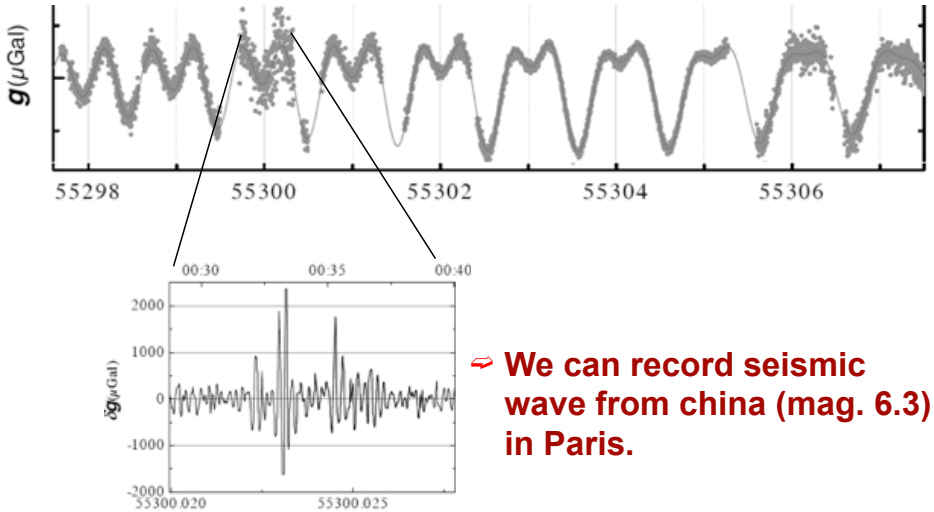

- **We can record seismic wave from china (mag. 6.3) in Paris.**

Sensitivity to rotations

- When the light pulses used for beam-splitter and mirrors are also separated in space, the paths enclose an area A.
- the interferometer phase is then also sensitive to the rotation Ω of the plane of the IFM, like for the Sagnac effect in optics.
- the phase shift depends on the de Broglie wavelength of the atom λ_{dB} and of the velocity v_l of the atom along the main direction of the beam like

$$\delta\psi_{rot} = \frac{4\pi}{\lambda_{dB} v_l}\Omega.A$$

- for 3 laser waves separated by a distance L, $A = L^2 v_{rec}/v_l$ and the phase shift can be recast into

$$\delta\psi_{rot} = \vec{k}_{eff}.\vec{a}\left(\frac{L}{v_l}\right)^2 + \Delta\phi$$

with $\vec{a} = -2\vec{\Omega} \times \vec{v}$ the Coriolis acceleration.

velocity sensor configuration to measure the photon-recoil

The objective of the photon-recoil measurement is an experimental value for the fine-structure constant α.

$$\alpha^2 = \frac{2R_\infty}{c}\frac{m_{at}}{m_e}\frac{h}{m_{at}}$$

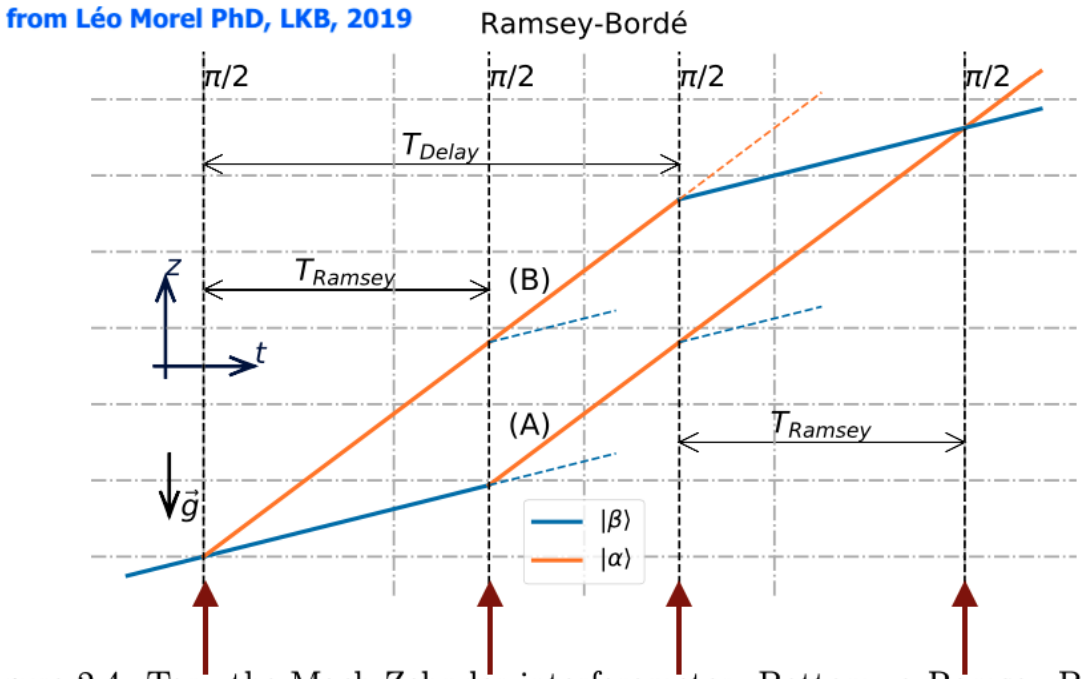

Figure 2.4: Top: the Mach Zehnder interferometer. Bottom: a Ramsey Bordé interferometer in differential velocity sensor configuration. The black vertical dashed lines indicates the optical pulses with their associated pulse area. The colored lines display the atomic trajectories. The dashed colored lines show the loss channels.

velocity sensor configuration to measure h/M

The trajectory of the atoms is controlled by Bloch oscillation in an optical lattice which transfers an integer number of recoil-velocity $v_r = \hbar k/m$. This latest results were based on the transfer of $1000\hbar k$ and reached a relative uncertainty for α of 8.1×10^{-11}.

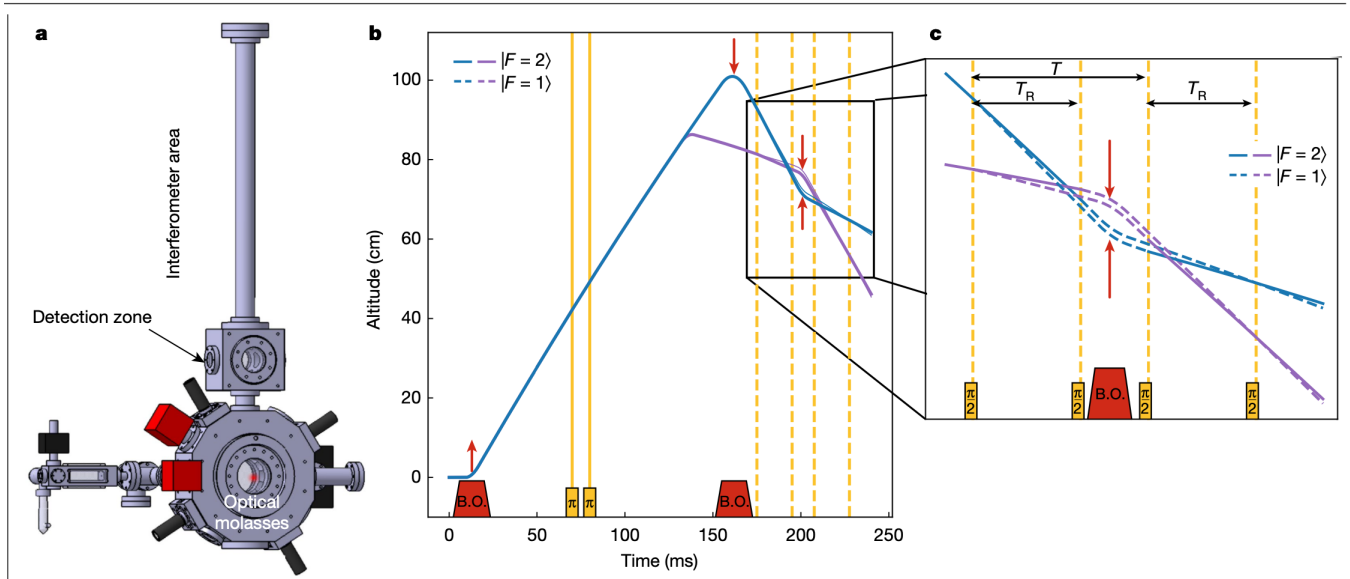

Fig. 2 | Experimental setup. a, Design of the vacuum chamber; the atom interferometer—a 70-cm-long magnetically shielded tube—is located in the upper area. **b**, Sequence of Bloch oscillations (B.O., red) and Raman pulses (yellow) used to control the trajectory of atoms before starting the atom interferometer. **c**, Atom interferometer light pulse sequence. The atomic trajectories for upward (blue) and downward (purple) accelerations are previously calculated to mitigate the gravity gradient effect. The separation between the two paths of each interferometer is exaggerated for clarity.

Morel *et. al* nature **588** (2020) p61.

Interferometer based on material gratings

- typical diffraction grating period : 200 nm, $\theta_{diff} = \lambda_{dB}/d_g \simeq$ mrad
- like in photon-optics, the diffraction is induced by a periodic modulation of the wavefront (no internal state involved)
- it does not rely on a resonant light-matter interaction

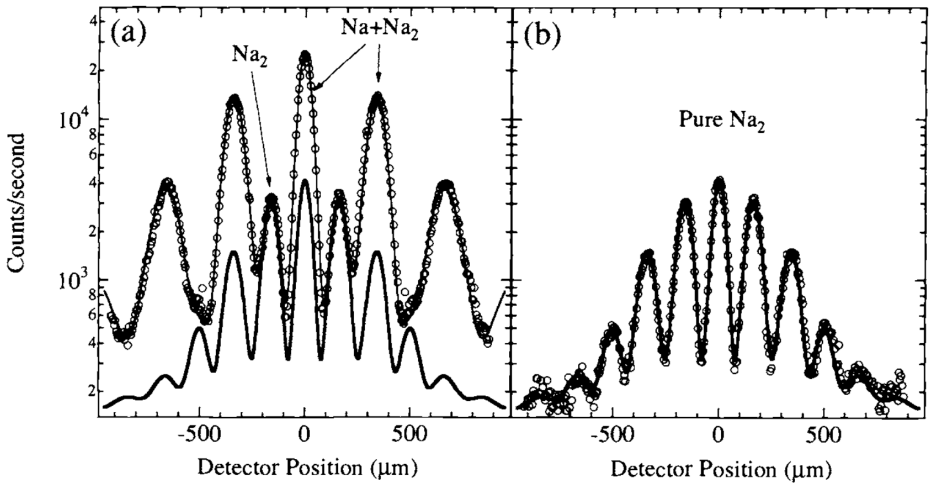

FIG. 6. Diffraction of 750 m/sec sodium atoms and molecules (Kr as a carrier gas) by a 100 nm period nanofabricated diffraction grating: (a) Diffraction of the mixed atom–molecule beam (deflecting laser off). One can clearly distinguish the atoms from the Na_2 molecules by their different diffraction angle. A fit to the combined diffraction pattern (thin solid line) indicates 16.5% of the intensity is molecules. The thick solid line is the fit to the Na_2 diffraction pattern in (b). For this measurement the deflecting laser was on. The fits determine the grating open fraction to be 30% and are a very good measurement (<.1%) of the de Broglie wavelength (velocity) of the atomic/molecular beam.

Pritchard and coll,1992

Interferometer based on material gratings

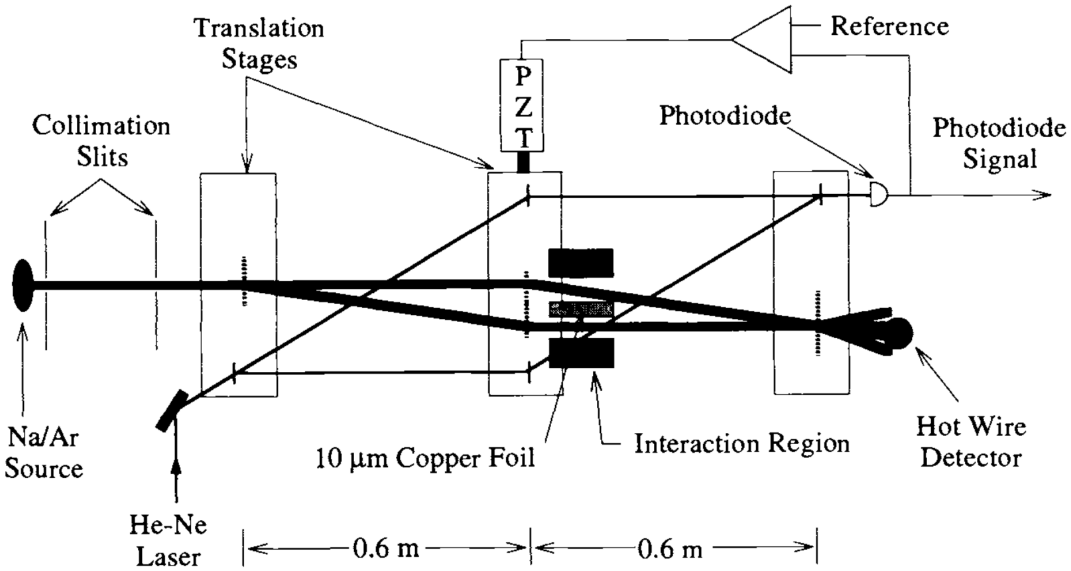

FIG. 9. A schematic, not to scale, of our atom interferometer (thick lines are atom beams). The 0th and 1st order beams from the first grating strike the middle grating where they are diffracted in the 1st and −1st orders. These orders form an interference pattern in the plane of the third grating, which acts as a mask to sample this pattern. The detector, located beyond the third grating, records the flux transmitted through the third grating. The 10 cm long interaction region with the 10 μm thick copper foil between the two arms of the interferometer is positioned behind the second grating. An optical interferometer (thin lines are laser beams) measures the relative position of the 200 nm period atom gratings (which are indicated by vertical dashed lines). Pritchard and coll, 1991

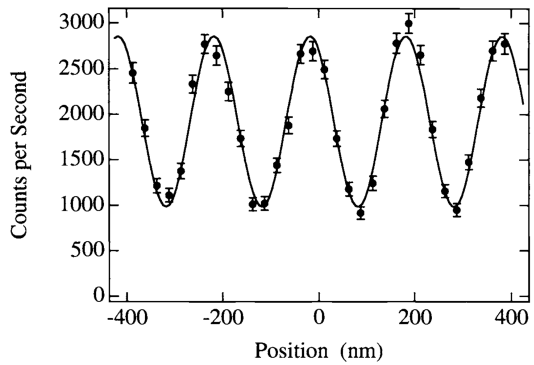

FIG. 10. Interference pattern from 30 sec of data (1 sec per point). The contrast is 49% and the phase uncertainty is <10 mrad.

Phases in interferometers

OPTICS AND INTERFEROMETRY WITH ATOMS AND MOLECULES

JÖRG SCHMIEDMAYER, MICHAEL S. CHAPMAN, CHRISTOPHER R. EKSTROM, TROY D. HAMMOND, DAVID A. KOKOROWSKI, ALAN LENEF, RICHARD A. RUBENSTEIN, EDWARD T. SMITH, and DAVID E. PRITCHARD

Department of Physics and Research Laboratory for Electronics, Massachusetts Institute of Technology, Cambridge, Massachusetts

To understand the principles of our interferometer, it is helpful to review the theoretical foundations of matter wave interferometry using semi-classical physics. We begin by considering the difference in phase between two possible paths Γ_1 and Γ_2 through the interferometer from source to detector, since this difference determines the phase of the interference pattern. The difference between the phases accumulated along each path can be expressed in terms of the classical actions along these paths $S_{1,2}$ (Feynman and Hibbs 1965; Storey and Cohen-Tannoudji, 1994):

$$\varphi = \frac{1}{\hbar}\,(S_1 - S_2). \tag{1}$$

The classical action is defined in terms of the Lagrangian, which is (for a one-dimension system with a position-dependent potential)

$$L(x, \dot{x}) = \tfrac{1}{2}\, m\dot{x}^2 - V(x) \tag{2}$$

for a particle with mass m in a potential $V(x)$. The classical action along each path then becomes (for $i = 1,2$)

$$\begin{aligned} S_i &\equiv \int_{\Gamma_i} L[x(t),\dot{x}(t)]\,\mathrm{d}t \\ &= \int_{\Gamma_i} \left(mv\,\frac{\mathrm{d}x}{\mathrm{d}t} - \left[V(x) + \frac{mv^2}{2} \right] \mathrm{d}t \right) \\ &= \int_{\Gamma_i} (p\,\mathrm{d}x - H\,\mathrm{d}t) \end{aligned} \tag{3}$$

where H is the Hamiltonian governing the classical motion of the particle. In a time-independent problem, H is constant and the phase difference accumulated along the classical paths can be written as

$$\varphi = \int_{\Gamma_1} k_1(x)\,\mathrm{d}x - \int_{\Gamma_2} k_2(x)\,\mathrm{d}x \tag{4}$$

where $k(x) = \frac{1}{\hbar}\sqrt{2m(E - V(x))}$ is the local k vector.

Phases in interferometers

paths: that is, $\varphi = \varphi_{\text{position}} + \Delta\varphi$. The first phase contribution, hereafter referred to as the *position* phase, is a function of the relative transverse grating positions, x_i, given by

$$\varphi_{\text{position}} = \frac{2\pi}{d_g}(x_1 - 2x_2 + x_3) = k_g(x_1 - 2x_2 + x_3) \tag{5}$$

where $k_g = 2\pi/d_g$ is the lattice vector of the grating. The second or *interaction* phase shift ($\Delta\varphi$) arises from the difference between the interactions along the two paths:

$$\Delta\varphi = \frac{1}{\hbar}\int_{\Gamma_1^0} \mathrm{L[x(t),\dot{x}(t)]}\,\mathrm{d}t - \frac{1}{\hbar}\int_{\Gamma_2^0} L[x(t),\dot{x}(t)]\,\mathrm{d}t \tag{6}$$

where Γ_1^0 and Γ_2^0 now denote classical paths through the interferometer with $x_1 = x_3 = 0$ and with no applied interaction. This split is allowed because the action is stationary with respect to small perturbations of the paths. By splitting the observed phase in this manner, we can focus our attention on analyzing the phase difference between just the two paths Γ_1^0 and Γ_2^0 rather than solving the full path integral problem (Feynman and Hibbs, 1965). It is important to note here that $\Delta\varphi$ is 0 when the action along both paths are equal; that is, only a difference in the applied potential $V(x)$ along the two paths will lead to an *interaction* phase shift $\Delta\varphi$.

A limit to matter-wave interferometry?

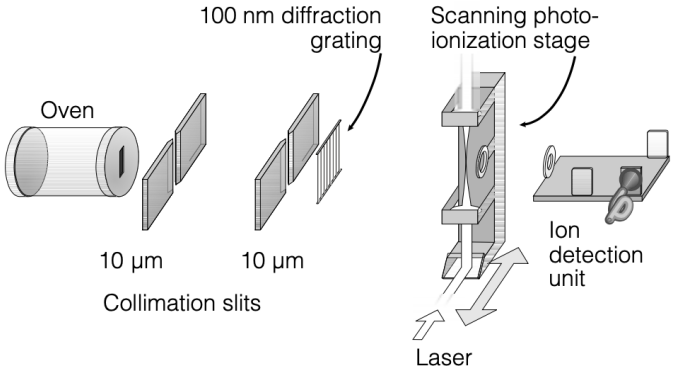

Figure 1 Diagram of the experimental set-up (not to scale). Hot, neutral C_{60} molecules leave the oven through a nozzle of 0.33 mm × 1.3 mm × 0.25 mm (width × height × depth), pass through two collimating slits of 0.01 mm × 5 mm (width × height) separated by 1.04 m, traverse a SiN_x grating (period 100 nm) 0.1 m after the second slit, and are detected via thermal ionization by a laser 1.25 m behind the grating. The ions are then accelerated and directed towards a conversion electrode. The ejected electrons are subsequently counted by a Channeltron electron multiplier. The laser focus can be reproducibly scanned transversely to the beam with 1-μm resolution.

680

© 1999 Macmillan Magazines Ltd

NATURE | VOL 401 | 14 OCTOBER 1999 | www.nature.com

Wave–particle duality of C_{60} molecules

Markus Arndt, Olaf Nairz, Julian Vos-Andreae, Claudia Keller, Gerbrand van der Zouw & Anton Zeilinger

Institut für Experimentalphysik, Universität Wien, Boltzmanngasse 5, A-1090 Wien, Austria

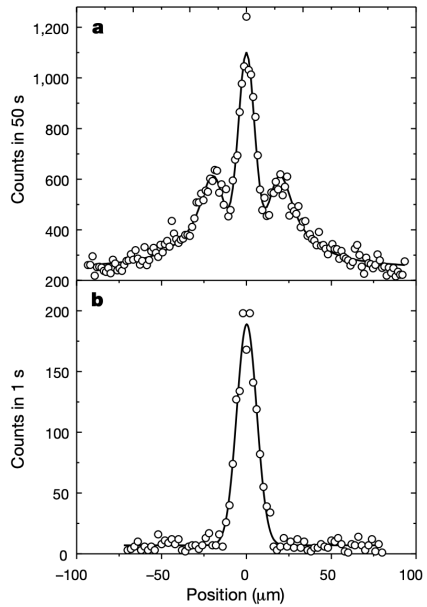

Figure 2 Interference pattern produced by C_{60} molecules. **a**, Experimental recording

What's new about optical clock

- optical clocks now reach amazing stability and precision.
- the best instability, of the order of 10^{-16} after 1 second of averaging, is 2 orders of magnitude better than for micro-wave clock. It is reached by optical clock based on Strontium neutral atoms trapped in an optical lattice, taking advantage once again of the Lamb-Dicke effect.

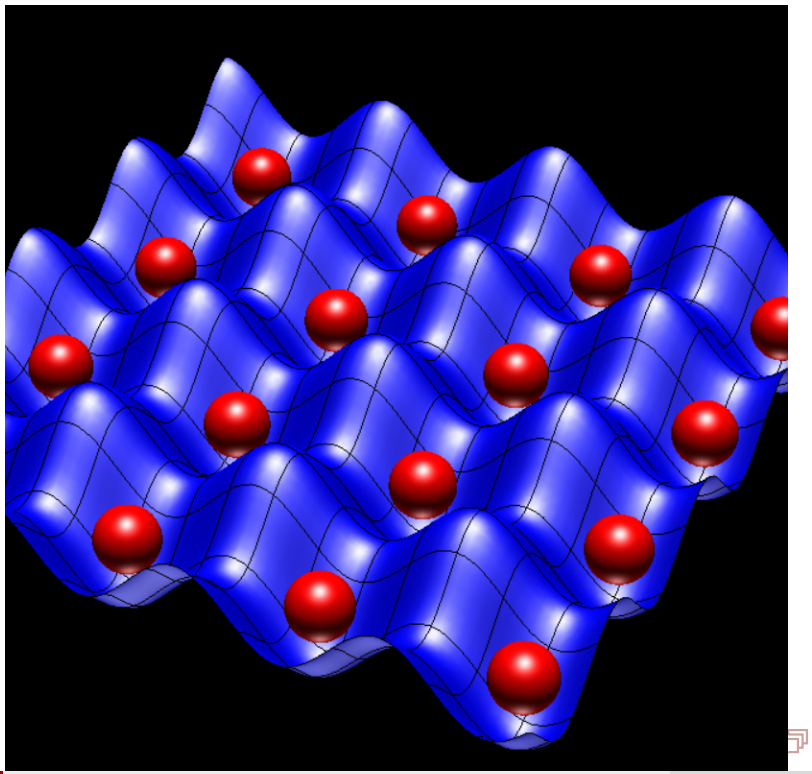

An optical clock based on entangled atoms

- the lowest systematic uncertainty, or the best accuracy, just lower than 10^{-18} is reached by an optical clock based on a single Al^+ ion, co-trapped with a partner-ion in a radio-frequency trap (or Paul trap).

The trap of NIST's quantum logic clock is the gold structure with the cross-shaped cutout. (credit S. Burrows-JILA)
The two ions share the same vibration mode within the trap

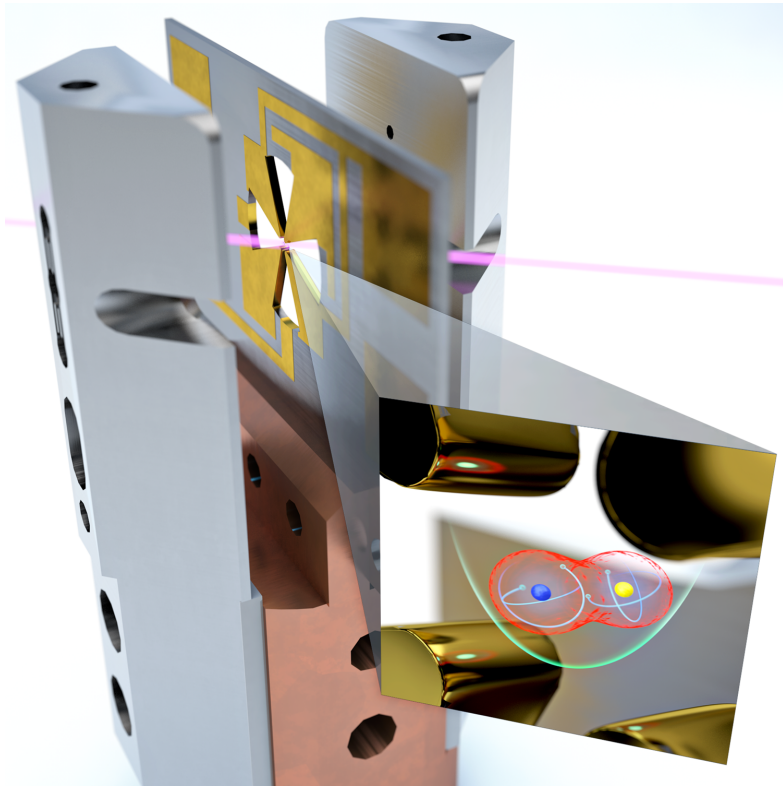

An optical clock based on entangled atoms

- Al^+ ion is a good candidate for a support for an optical clock but a bad candidate for efficient cooling and state-detection
- it is trapped with a partner Mg^+ ion with a strong coupling with laser light.
- the internal state of the two ions are entangled to their collective vibrational modes to create an entangled state for the two ion internal state and process "quantum logic spectroscopy".
- a series of laser pulses transfers the information in the Al^+ system first to a collective motional state then to the Mg^+ internal state followed by Mg^+ detection

Perspectives?

- devices taking advantage of the quantum properties of particles reach very high precision which will help testing our models for physics, and may bring new insight into quantum physics itself.
- a lot of exciting results and discussions ahead of us.

How to reduce the atomic velocity ?

Make sure that the atom absorbs a counter-propagating photon!!

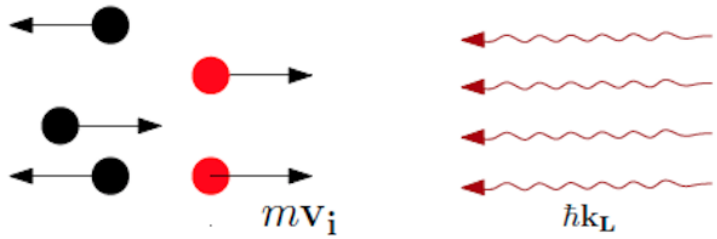

- The Doppler effect shifts the laser frequency *seen* by the atoms :

$$\omega_L^{at} = \omega_L - \mathrm{k}_L.\mathrm{v}$$

- Transition occurs if energy and momentum are conserved :

$$\mathrm{p} + \hbar\mathrm{k}_L = \mathrm{p}' \quad (21)$$

$$E_g + \hbar\omega_L + \mathrm{p}^2/2m = E_e + (\mathrm{p}')^2/2m \quad (22)$$

it induces

$$\omega_L - \mathrm{k.v} = \omega_L^{at} = \omega_0 + \hbar\mathrm{k}_L^2/2m$$

- If $\omega_L < \omega_0$, it takes $\mathrm{k.v} < 0$ for ω_L^{at} to reach the atomic resonance then $||\mathrm{p}'|| < ||\mathrm{p}||$.

orders of magnitude

- $\hbar^2 k_L^2/2m = \hbar\omega_{rec}$ is the recoil energy, of the order of few 10 kHz
- for Doppler laser cooling, strong dipolar transitions are used (natural linewidth $\simeq$ 10 MHz)
- The recoil energy is often not taken into account in Doppler laser cooling and the conservation conditions reduce to

$$\omega_L - k.v = \omega_L^{at} = \omega_0$$

  The choice of $\omega_L < \omega_0$ controls the velocity range in resonance with the excitation.
- To optimise the efficiency and control the limit temperature, one must go back to the fundamental of atom-laser interaction.

Looking inside the radiation pressure force

the force on a atom is $\Delta p/\Delta t = \hbar k_L \times N_\phi(\Delta t)$

recoil induced by the absorption of one photon	$\times$	number of photons scattered spontaneously during Δt

$$N_\phi(\Delta t) = (\Gamma \times \Delta t) \times P_e$$

probability for an atom to emit spontaneously a photon during Δt when in the excited state ($\Gamma = 1/\tau_e$)	$\times$	probability for an atom to be in the excited state P_e

to control the force, one needs to know how to control P_e :

$$F = \hbar k_L \times \Gamma \times P_e$$

the two-level atom in a laser electric field

- $|g\rangle, |e\rangle$ are the two involved atomic states, with energy defined by $E_e - E_g = \hbar\omega_0$ and $\omega_L \simeq \omega_0$.
- without any laser field, the hamiltonian of an atom at rest is

$$\hat{H}_0 = \frac{\hbar\omega_0}{2}\left(|e\rangle\langle e| - |g\rangle\langle g|\right)$$

- atoms do not have any permanent dipole, but the oscillating electric field induces one
- within the **dipolar approximation** ($\lambda_L \gg r_{at}$), the laser-atom interaction can be understood as the interaction between the electric field and the transition dipole $d_{e.g.}$:

$$V_{AL}(\mathrm{r}_{at}, t) = -\mathrm{d}_{eg}.\mathrm{E}_L(\mathrm{r}_{at}, t)$$

where r_{at} is the position of the atom center of mass.

the two-level atom in a laser electric field

- for an atom with a single active electron, and r_e its position operator, the dipole operator is

$$\mathrm{d} = -q_e \mathrm{r}_e$$

- if the laser wave is a plane wave, with polarisation e_L

$$\mathrm{E}_L(\mathrm{r}_{at}, t) = E_L \mathrm{e}_L \cos(\omega_L t - \Phi(\mathrm{r}_{at}))$$

- the interaction strength driving the transition between $|g\rangle$ and $|e\rangle$ is represented by the Rabi frequency $\Omega_1(\mathrm{r}_{at})$

$$\langle e|V_{AL}(\mathrm{r}_{at}, t)|g\rangle = \hbar\Omega_1(\mathrm{r}_{at}) = -\langle e|\mathrm{d}.\mathrm{e}_L|g\rangle E_L \cos(\omega_L t - \Phi(\mathrm{r}_{at}))$$

the selection rules

- many symmetry properties control if $\langle e|\mathrm{d.e}_L|g\rangle \neq 0$

- The transition between Zeeman sub-levels M_J depends one the light polarization, relatively to the local magnetic field.
- This has to be considered when designing an experimental set-up.
  (to know more about selection rules, use an atomic physics book, like the one by Christopher Foot, *Atomic Physics* (Oxford master series in Physics))